

Composition of Melt Inclusions and Age of Zircons from Plagiogneisses of the Archean Complex in the Kola Superdeep Borehole, Baltic Shield

V. P. Chupin¹, V. R. Vetrin², N. V. Rodionov²,
D. I. Matukov³, N. G. Berezhnaya³, S. A. Sergeev³,
Academician of the RAS F. P. Mitrofanov², and Yu. P. Smirnov⁴

Received August 5, 2005

DOI: 10.1134/S1028334X06010363

The origin of zircon is of great importance for the petrological interpretation of U–Pb dates. Direct information on the magmatic origin of zircon from intensely metamorphosed Archean rocks is provided by findings of primary melt inclusions [1–3]. At the same time, not even detailed structural–morphological investigations are sufficient to decipher the relict-magmatic or later anatectic origin of zircon with melt inclusions. The timing of melt entrapment must be established for the reliable identification of these genetic types.

In this work, we report the first data on the timing of entrapment of different primary melts and fluid inclusions in accessory zircon from biotite trondhjemite plagiogneiss (Sample 26 from a depth of 10 780 m) taken from sequence VIII of the Archean complex in the Kola superdeep borehole (SG-3). The sequence located at the interval of 10 601–11 411 m consists of predominant biotite and subordinate amphibole–biotite plagiogneisses (~66%) and amphibolites (~23%) with interbeds of ferruginous quartzites [4]. It is believed that the oldest zircons (with an age of 2.83 Ga) from plagiogneisses of SG-3 formed during the crystalliza-

tion of the volcanic protolith [5], though some geologists attribute these old dates to the diaphoresis of granulites in amphibolite facies [6].

It should be noted that zircons from tonalite–trondhjemite gneisses at the base of the borehole are significantly less altered, demonstrating a better preservation of inclusions and minimum present-day loss of Pb as compared to the Archean zircons from their surface analogues [5, 7].

Zircons were studied in monofraction taken from Sample 26. Based on optical investigations, zircon crystals were divided into morphological types, and primary melt and fluid inclusions were identified in them [8]. The chemical composition of glass inclusions was determined on a Camebax-micro microprobe at the Joint Institute of Geology, Geophysics, and Mineralogy. The timing of inclusion entrapment was constrained by high-resolution measurements of the isotope age of the host zircon (near the inclusion) on a SHRIMP II ion microprobe at the Center of Isotopic Research of the Karpinskii All-Russia Research Institute of Geology. U–Pb ratios were measured following the technique described in [9]. Obtained data were processed with a SQUID program [10]. Errors of single analyses are given at the 1 σ level. Concordia plots were constructed using an ISOPLOT/EX program [11]. The small beam size (25 \times 18 μ m, crater depth 3 μ m) made it possible to determine within the limits of individual error the age of zircon, which entrapped different melt and liquid CO₂ inclusions in the course of crystallization.

Two morphological types of zircon were distinguished in Sample 26. The predominant type is subeuhedral prismatic zircons with an elongation coefficient of 1.5–3.5, whereas complicatedly faceted isometric zircons are subordinate. Prismatic zircons are optically homogeneous. However, cathodoluminescence analysis revealed homogeneous short- or long-prismatic

¹ *Institute of Mineralogy and Petrography, Siberian Division, Russian Academy of Sciences, pr. Akademika Koptyuga 3, Novosibirsk, 630090 Russia; e-mail: chupin@uiggm.nsc.ru*

² *Geological Institute, Kola Scientific Center, Russian Academy of Sciences, ul. Fersmana 14, Apatity, Murmansk oblast, 184209 Russia; e-mail: vetrin@geoksc.apatity.ru*

³ *Center of Isotopic Research, Karpinskii All-Russia Research Institute of Geology, Srednii pr. 74, St. Petersburg, 199106 Russia; e-mail: cirvsg@vsegei.sp.ru*

⁴ *Kola Superdeep Scientific-Industrial Center, Zapolyarny, Murmansk oblast, 184415 Russia; e-mail: sd3kg1@com.mels.ru*

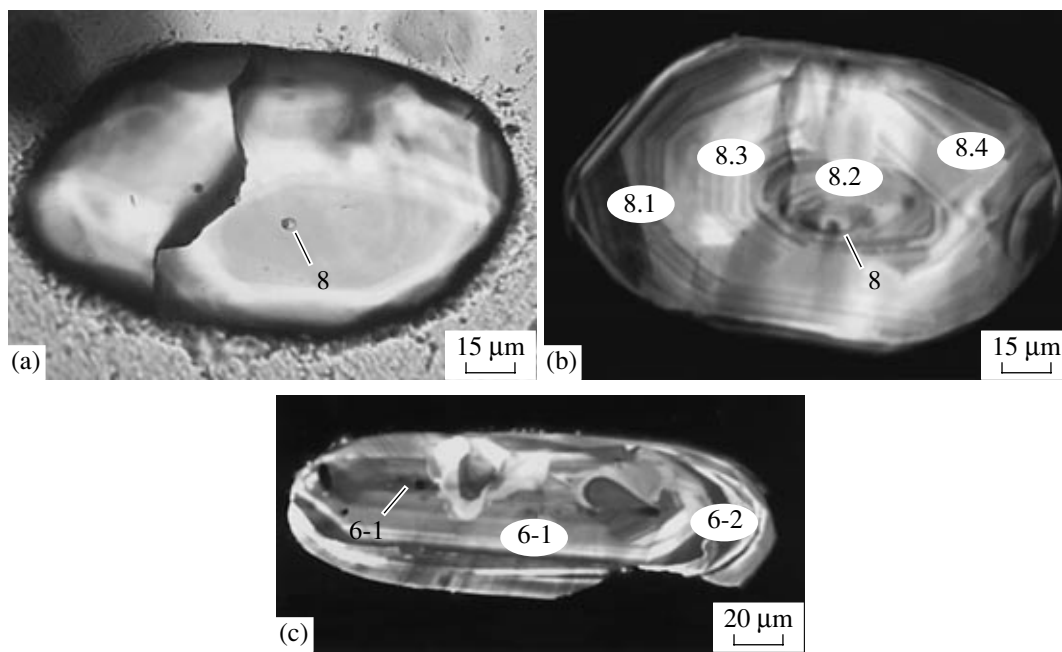


Fig. 1. Prismatic zircon crystals from Sample 26 with trondhjemite melt inclusions. Numbers near the inclusions (6-1, 8) correspond to the analysis numbers in Table 1. The oval shows the zircon area analyzed by ion microprobe. The number in the oval corresponds to the data point number in Table 2. (a) Image of crystal 8 in transmitted light; (b, c) cathodoluminescence images of crystals 8 and 6.

inner part of crystals replaced by zoned zircon in the intermediate and outer parts of the crystals (Fig. 1). Some zircons have an homogeneous overgrowth and strongly corroded core.

Primary melt inclusions occur in the prismatic zircons (Fig. 1) and are absent in the complicatedly faceted isometric grains. The inclusions are small—typically 2–6 µm long (occasionally, up to 14 µm). They consist of fine-grained silicate aggregate and interstitial fluid phase. The smallest inclusions (up to 2–3 µm in size) consist of an optically homogeneous isotropic phase (possibly, glass).

The glasses of heated and subsequently quenched inclusions in the central parts of crystals have mainly Na-rhyodacite and plagioryholite compositions, while glasses of inclusions located closer to the rim have rhyolite (with increased K content) compositions (Table 1). In the Ab–An–Or classification diagram [12], inclusions from the central parts of crystals are mainly plotted in the trondhjemite field, whereas melt inclusions from intermediate parts and rims correspond to granites.

Central homogeneous parts of prismatic zircons occasionally contain single primary inclusions of liquid CO₂ that are syngenetic with melt inclusions. The presence of such inclusions indicates the crystallization of early zircons in the deep-seated magma chamber from CO₂-saturated magmas under a separating fluid pressure of 3.5 kbar [8].

Results of the U–Pb dating of prismatic zircons from Sample 26 are presented in Table 2 and Fig. 2. According to [7], if U–Pb datings are concordant, then

²⁰⁷Pb/²⁰⁶Pb ages are the most precise dates for Precambrian rocks. The old ²⁰⁷Pb/²⁰⁶Pb age values (nine determinations with the degree of discordance equal to 0) obtained for the central and intermediate parts of studied zircons form an uninterrupted and overlapping (within the limits of measurement error) time interval from 2865 to 2813 Ma. Taking into account zircon ages with a discordance of 1 (central parts of crystals 34 and 8), the old value of this interval was presumably more than 2887 Ma.

The presence of primary melt inclusions in the prismatic crystals suggests the magmatic origin of host zircon. Judging from the ²⁰⁷Pb/²⁰⁶Pb age (2842 ± 13 Ma for crystal 7 and older ages for crystals 6 and 8 in Table 2), zircon centers with trondhjemite (plagioryhodacite and plagioryholite) melt inclusions are ascribed to the earliest generation of primary magmatic zircon. The presence of glass inclusions in the central parts of prismatic crystals suggests that the zircons represent primary magmatic mineral of volcanic protolith of gneisses.

The central parts of concordant, oldest zircons (crystals 7, 8, and 31–34) have low U and Th contents (on average, 146 and 58 ppm, respectively) and similar Th/U ratios (on average, 0.40). The presence of trondhjemite melt inclusions in zircons 7.1 and 8.2 indicates that the geochemistry of this group is typical of old zircons derived from the Na-saturated acid melts. The crystal 6 (Fig. 1c) with plagioryhodacite inclusion in the central part (6-1 in Table 1) also belongs to the oldest zircons. The intermediate part of this crystal contains trachyrhyolite inclusion (6-2 in Table 1). Host zircon

Table 1. Chemical composition (wt %) of the rock and glasses of heated melt inclusions in zircon of biotite plagiogneisses (Sample 26) from the Kola superdeep borehole

Inclusion no.	SiO ₂	TiO ₂	Al ₂ O ₃	FeO	MgO	CaO	Na ₂ O	K ₂ O	Cl	F	Total	HfO ₂ *	Location**	K ₁	K ₂
1	68.64	0.32	13.17	4.01	0.76	4.19	3.22	2.66	0.07	0.09	97.13	0.75	c	0.83	0.84
2	70.57	0.35	10.97	3.94	0.72	4.59	3.22	3.68	0.09	0.05	98.13	0.70	c-i	1.14	0.62
3	69.17	0.23	12.99	5.07	1.21	1.06	2.91	4.17	0	0.08	96.81	0.90	r	1.43	1.16
4	72.64	0.07	14.58	0.12	0.03	1.39	4.89	2.46	0	n/a	96.18	1.00	c-i	0.50	1.10
5	74.92	0.05	12.05	0	0	0.63	3.67	2.93	0	"	94.25	1.05	i	0.80	1.17
6-1	72.81	0.17	13.68	0.1	0.02	1.84	5.12	2.28	0.01	"	96.03	1.00	c	0.45	0.96
6-2	74.99	0.57	11.09	1.23	0.04	0.59	3.99	5.02	0	"	97.52	0.96	c	1.26	0.85
7	73.39	0.10	14.04	0.29	0.08	1.48	4.74	1.71	0	"	95.83	0.84	c	0.36	1.14
8	74.59	0	13.74	0.55	0	1.85	3.83	1.02	0	"	95.58	0.87	c	0.27	1.27
9	72.03	0.02	15.53	0.14	0.01	1.23	3.43	3.37	0	0	95.76	1.00	r	0.98	1.35
10	75.18	0	12.73	0.24	0	1.56	3.32	2.78	0	n/a	95.81	1.15	i	0.84	1.13
11	77.07	0.03	8.98	0.01	0.02	0.73	2.85	2.72	0	"	92.41	0.96	i	0.95	1.00
12	73.31	0	13.77	0.19	0	1.55	2.69	3.77	0	0	95.28	1.25	i	1.40	1.22
13	73.33	0.27	14.95	2.17	0	1.11	0.69	2.92	0	n/a	95.44	1.21	r	4.23	2.80
14	76.79	0.07	14.25	0.22	0.09	0.27	1.98	4.14	0.01	0	97.82	1.08	r	2.10	1.73
15	71.20	0.29	15.17	2.27	0.67	2.81	5.26	1.38	n/a	n/a	99.58			0.26	1.00

Note: (1–14) Inclusions; (15) bulk composition of the rock (Sample 26) determined at the Geological Institute, Kola Scientific Center; (n/a) not analyzed. (*) Content of HfO₂ in zircon near the inclusion; (**) location of inclusions in the crystal: (c) central part, (i) intermediate part, (r) rim. Analyses (1–3), (4, 5), and (6-1, 6-2) are from three individual crystals, in which inclusions 1, 2, 4, and 6-1 are located closer to the central part, while inclusions 3, 5, and 6-2 are closer to the rim. High contents of FeO (analyses 1–3) and CaO (analyses 1 and 2) are related to the presence of xenogenic micrograins (phenocrysts) of magnetite and, possibly, apatite in the inclusions. $K_1 = K_2O/Na_2O$; $K_2 = A/CNK = \text{mol Al}_2\text{O}_3/(\text{CaO} + \text{Na}_2\text{O} + \text{K}_2\text{O})$.

(6.1 in Table 2) has significantly higher Th (226 ppm) and U (353 ppm) contents as compared to the average contents of these elements in zircons with trondhjemite inclusions.

The oldest zircons that crystallized from trondhjemite melts are geochemically similar to the relatively “young” concordant zircons (34.2, 35.1, 37.2 from intermediate parts and 36.1 from the central part of crystals, with average U and Th contents of 129 and 21 ppm, respectively), indicating their crystallization from similar melts. The minimum age of the young primary magmatic zircons is 2813 ± 8 Ma.

The nearly concordant ²⁰⁷Pb/²⁰⁶Pb age of the intermediate zone of zircon, the central part of which contains fluid CO₂ inclusion (syngenetic to the melt inclusions), is 2856 Ma (crystal 23.1, Table 2), indicating that this zircon belongs to primary magmatic zircons of the early generation. The geochemistry of this crystal is very similar to that of the oldest zircons crystallizing from trondhjemite melts.

Zircons with rhyolite inclusion (crystal 10, Table 1) in the intermediate part have a nearly concordant age of ~2812 Ma (10.3, Table 2). This zircon is presumably ascribed to the later generation of protolithic zircons

with respect to the early zircons with fluid CO₂ inclusions and trondhjemite melt inclusions. Zircon from the intermediate part of the crystal (10.2, Table 2) has high U and Th contents. The high U and Th contents in the intermediate parts of crystals 11 (with rhyolite inclusion) and 38 indicate that they represent the youngest protolithic zircons.

The youngest concordant age (2589 ± 19 Ma) was obtained from the outer part of the elongated prismatic zircon having strongly corroded magmatic core with an age of 2846 ± 8 Ma (crystal 33, Table 2). The outer part consists of at least two shells that fall within the analyzed area. Therefore, the obtained age values can be interpreted as the averaged age of these shells. The outer shell was presumably formed during the latest metamorphic transformations. The crystallization age of gneisses of sequence VIII of the Archean Complex in the Kola superdeep borehole presumably corresponds to dates of the complicatedly faceted isometric zircons of presumably metamorphic origin [8]. One such crystal (crystal 25, Table 2), ~25 μm in size, defines a concordant age of 2675 ± 7 Ma.

The complex study of melt inclusions and SHRIMP dating of zircons from trondhjemite gneisses of

Table 2. U–Pb isotope data (SHRIMP II ion microprobe) on prismatic zircons in biotite plagiogneiss (Sample 26) from the Kola superdeep borehole

Analysis no.	$^{206}\text{Pb}_c$, %	Concentration, ppm			Th/U	Isotope ratios		Isotope age, Ma $\pm 1\sigma$	<i>Rho</i>	Degree of discordance, %
		U	Th	$^{206}\text{Pb}^*$		$^{207}\text{Pb}^*/^{235}\text{U} \pm \%$	$^{206}\text{Pb}^*/^{238}\text{U} \pm \%$			
24.1 c	–	107	28	49.7	0.26	15.38 \pm 2.00	0.5407 \pm 1.50	2877 \pm 21	0.75	3
23.1 i	0.12	220	75	105.0	0.34	15.54 \pm 1.50	0.5532 \pm 1.30	2856 \pm 12	0.87	1
8.1 r + i	–0.01	385	207	180.0	0.56	15.23 \pm 0.86	0.5426 \pm 0.76	2855 \pm 6.5	0.89	2
8.2 c	–0.02	148	57	70.5	0.40	15.77 \pm 1.00	0.5553 \pm 0.85	2874 \pm 9.4	0.83	1
8.3 i + c	0.09	74	25	34.8	0.35	15.50 \pm 1.30	0.5464 \pm 1.10	2872 \pm 13	0.80	2
8.4 i	0.00	69	22	32.5	0.33	15.32 \pm 1.30	0.5496 \pm 1.00	2844 \pm 12	0.81	1
6.1 i + c	–	353	225	167.0	0.64	15.51 \pm 1.10	0.5493 \pm 0.97	2865 \pm 9	0.87	2
6.2 i	–	871	44	413.0	0.04	15.39 \pm 0.86	0.5519 \pm 0.77	2845 \pm 6	0.90	0
7.1 c	0.09	168	95	79.8	0.57	15.36 \pm 1.60	0.5514 \pm 1.40	2842 \pm 13	0.87	0
10.3 c + i	0.19	238	102	113.0	0.44	15.13 \pm 1.30	0.5535 \pm 1.10	2812 \pm 11	0.84	–1
10.2 i	0.10	935	177	453.0	0.19	14.94 \pm 1.00	0.5639 \pm 0.85	2761 \pm 9	0.85	–4
11.1 i	0.02	505	339	246.0	0.67	15.90 \pm 1.00	0.5674 \pm 0.88	2853 \pm 8	0.88	–2
11.2 r + i	–	414	31	174.0	0.07	13.10 \pm 1.90	0.4909 \pm 1.80	2772 \pm 11	0.94	7
31.1 c	0.02	271	83	130.0	0.31	15.72 \pm 1.70	0.5568 \pm 1.60	2865 \pm 7	0.97	0
32.1 c	0.19	54	17	26.2	0.31	15.71 \pm 2.10	0.5590 \pm 1.90	2856 \pm 16	0.89	0
32.2 i	0.03	532	232	259.0	0.44	15.89 \pm 1.60	0.5672 \pm 1.60	2852 \pm 5	0.98	–2
33.1 c	0.00	187	69	89.7	0.37	15.57 \pm 1.70	0.5579 \pm 1.60	2846 \pm 8	0.96	0
33.2 r	0.64	82	3	34.9	0.04	11.74 \pm 2.10	0.4918 \pm 1.80	2589 \pm 19	0.84	0
34.1 c + i	0.02	48	24	22.9	0.50	15.88 \pm 2.10	0.5550 \pm 1.90	2887 \pm 15	0.89	1
34.2 i	0.10	65	16	30.7	0.25	15.19 \pm 2.00	0.5500 \pm 1.80	2829 \pm 14	0.90	0
35.1 i	4.08	98	37	48.5	0.38	15.22 \pm 3.40	0.5515 \pm 1.80	2827 \pm 46	0.54	0
35.2 r	0.52	34	7	16.0	0.21	14.96 \pm 2.50	0.5510 \pm 2.10	2801 \pm 24	0.81	–1
36.1 c	–	165	21	77.7	0.13	15.16 \pm 2.20	0.5500 \pm 2.10	2824 \pm 12	0.94	0
37.1 c	1.08	896	26	448.0	0.03	15.76 \pm 1.80	0.5756 \pm 1.60	2814 \pm 14	0.88	–4
37.2 i	–	189	11	88.6	0.06	14.92 \pm 1.70	0.5452 \pm 1.70	2813 \pm 8	0.96	0
38.1 i	–	928	191	444.0	0.21	15.20 \pm 1.60	0.5572 \pm 1.60	2809 \pm 4	0.99	–2
38.2 r + i	0.02	69	11	30.9	0.16	14.17 \pm 2.00	0.5193 \pm 1.80	2809 \pm 14	0.91	4
39.1 i	0.04	250	91	115.0	0.36	14.26 \pm 1.70	0.5341 \pm 1.60	2773 \pm 8	0.96	1
25**	0.27	711	49	315.0	0.07	12.95 \pm 0.79	0.5148 \pm 0.68	2675 \pm 7	0.86	0

Note: Zircon crystals with inclusions: (24 and 23) liquid CO₂; (6–8) trondhemite melt; (6, 10, and 11) granite melt. Numbers of crystals with melt inclusions correspond to the analysis numbers in Table 1; (c, i, r) central part, intermediate part, and rim, respectively, of the crystals; (Pb_c, Pb*) total and radiogenic Pb, respectively; (25**) complicatedly faceted isometric zircon from Sample 39861 (plagiogneiss from a depth of 10 870 m); (*Rho*) correlation coefficient of $^{207}\text{Pb}^*/^{235}\text{U} - ^{206}\text{Pb}^*/^{238}\text{U}$ ratios.

sequence VIII of the Kola superdeep borehole has revealed the presence of old primary magmatic crystals with an age of up to 2887 \pm 15 Ma. This is not consistent with the previous view according to which the oldest zircons from the Archean Complex in SG-3 are products of granulite metamorphism. Primary magmatic zircons of early generation (from 2887 to 2842 Ma) formed in deep-seated magma chambers during the partial crystallization of CO₂-saturated trondhemite

magmas. The younger zircons (with an age of up to 2813 Ma) presumably also crystallized from deep-seated trondhemite melts. Rapid disequilibrium crystallization during effusion led to the formation of interstitial aggregates of residual SiO₂- and K₂O-saturated melts, which were entrapped as inclusions at the final crystallization stages of the protolithic zircons.

Such a long-term (70 Ma) zircon crystallization in the deep-seated magma chambers is consistent with

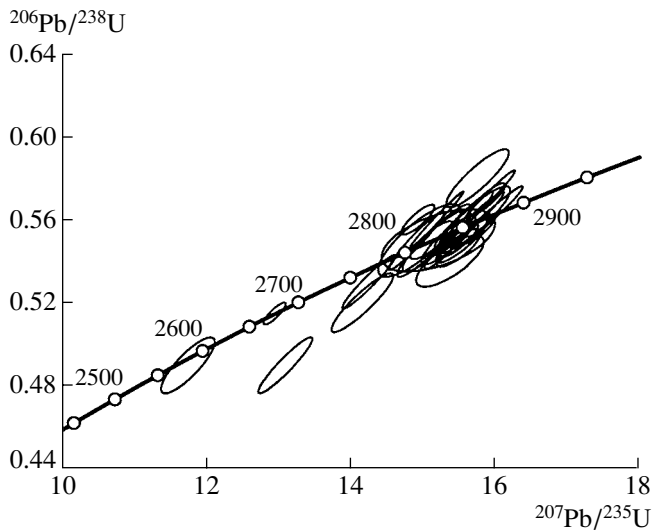


Fig. 2. Concordia diagram for zircons from biotite plagiogneisses (Sample 26) from the Kola superdeep borehole (ion microprobe data).

estimates on the duration of the generation of tonalite–trondhjemite–granite melts through the partial melting of mafic rocks [13].

ACKNOWLEDGMENTS

This work was supported by the Russian Foundation for Basic Research (project nos. 02-05-65074 and 02-05-64394).

We have contributed this paper to the IGCP-408 project (Comparison of the Composition, Structure, and Physical Properties of Rocks and Minerals in the Kola Superdeep Borehole and Their Analogues on the Surface).

REFERENCES

1. V. P. Chupin, A. V. Titov, L. M. Stepanyuk, *et al.*, Dokl. Akad. Nauk SSSR **323**, 545 (1992).
2. V. P. Chupin, S. V. Chupin, L. N. Pospelova, *et al.*, Dokl. Akad. Nauk SSSR **338**, 806 (1994).
3. S. V. Chupin, V. P. Chupin, J. M. Barton, *et al.*, Eur. J. Mineral. **10**, 1241 (1998).
4. *The Kola Superdeep Borehole. Scientific Results and Experience in the Study*, Ed. by V. P. Orlov and N. P. Laverov, (MF Tekhnoneftegaz, Moscow, 1998), pp. 59–70 [in Russian].
5. G. G. Duk, T. V. Kol'tsova, E. V. Bibikova, *et al.*, in *Isotope Geochronology of the Precambrian* (Nauka, Leningrad, 1989), pp. 72–86 [in Russian].
6. E. V. Bibikova, V. R. Vetrin, T. I. Kirnozova, *et al.*, Dokl. Akad. Nauk SSSR **332**, 360 (1993).
7. V. P. Chupin and V. R. Vetrin, Geokhimiya, No. 2, 1 (2005) [Geochem Int., No. 2, (177) 2005].
8. I. S. Williams, Rev. Econ. Geol. **7**, 1 (1998).
9. K. R. Ludwig, Berkley Geochronol. Center Spec. Publ., No. 1a (1999).
10. K. R. Ludwig, Berkley Geochronol. Center Spec. Publ., No. 2 (2000).
11. F. Barker, in *Trondhjemites, Dacites, and Related Rocks* (Elsevier, Amsterdam, 1979), pp. 1–12.
12. M. D. Jackson, K. Callagher, N. Petford, *et al.*, Lithos **79**, 43 (2005).